

gear

TECHNOLOGY®

SEP/OCT
2016

**software
savvy**

**FEA OF TOOTH FLANK FRACTURE
MANAGING SHOP FLOOR DATA**

**AGMA's Go-To Gear Guys
Advances in Spline Manufacturing**

Finite Element Analysis of Tooth Flank Fracture Using Boundary Conditions from LTCA

Baydu Al, Rupesh Patel and Paul Langlois

This paper demonstrates an application of the tooth interior fatigue fracture (TIFF) analysis method, as implemented in SMT's MASTA software, in which loaded tooth contact analysis (LTCA) results from a specialized 3-D contact model have been utilized to determine the load boundary conditions for analysis of tooth flank fracture (TFF). In contrast to existing TFF methods, which use analytical Hertzian contact stress formalisms, 2-D finite element analysis has been utilized. This method allows for the full stress field to be analyzed while retaining quick analysis times (compared to full finite element contact analysis) for the calculation of stress history and the estimation of residual stresses leading to fast optimization. This method also allows calculation of residual stresses by applying a transformation strain profile or the input of analytical profiles available in the open literature. This paper also demonstrates differences between the calculated stress profile based on MackAldener's methodology and an empirical calculation method initially proposed by Lang and adapted for TFF calculation. The paper reproduces TFF results obtained by Witzig using the described methodology and a reasonable agreement of the trends has been presented.

Introduction

Gears are case hardened to produce residual stresses at the surface, improving wear resistance, bending fatigue, and contact fatigue strength. These beneficial, compressive stresses are balanced by tensile stresses within the core. This poses an increased risk of fatigue crack initiation in the material below the surface. Both tooth flank fracture (TFF), also known as tooth flank breakage (TFB), and tooth interior fatigue fracture (TIFF), describe a failure mode where a subsurface fatigue crack initiates close to case core boundary, at approximately mid-height on the tooth. Previous research (Refs.1-8) has established that the direction in which the crack propagates and the appearance of the associated fracture is dependent on the flank loading (i.e. — single-stage loading vs. idler usage). Although there does not appear to be total agreement in the literature, TIFF (failure with reverse loading) and TFF (failure with single flank loading) appear to have very similar characteristics and crack initiation mechanisms. However, as shown in Figure 1, the final fracture shape is different, due to TIFF having near symmetric total stresses along the tooth centreline (with two possible initiation points per tooth).

Due to their similar characteristics both TIFF and TFF can be analysed using similar techniques. TIFF and TFF failures can appear at loads below the allowable loading conditions for pitting and bending fatigue failure modes based on internationally accepted calculation procedures (such as ISO 6336 (Ref.9) and AGMA 2101(Ref.10)). Therefore, an understanding of TIFF and TFF failure modes is required at the design

stage to avoid durability issues in the field. Previous research has shown that TFF and TIFF risk is dependent on the gear macro geometry, loading, and hardening properties. At this writing there is no currently standardized method to assess the probability of this type of failure and the relative importance of the influencing factors. It is worth noting, however, that TFF is an active topic within the ISO gearing committee that is currently working on a draft standard — ISO/DTR 19042 — for the calculation of tooth flank fracture performance.

In this paper we provide a brief summary of the current calculation methods found in the literature for both TFF and TIFF, as recently discussed in Al and Langlois (Ref. 11). The currently proposed approaches for TFF and TIFF all have similar, fundamental approaches consisting of four stages:

1. Calculation of stress history
2. Calculation of specification of residual stresses
3. Calculation of equivalent stresses using some fatigue criterion
4. Comparison with some initiation thresholds based on field experience or experiments

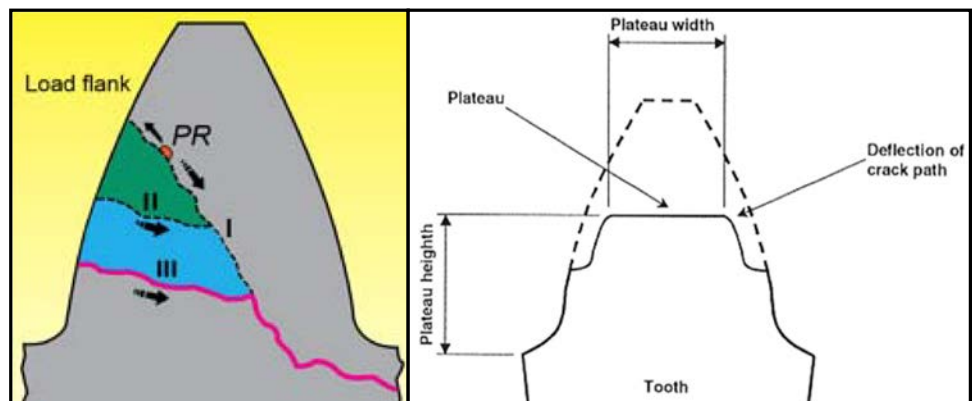


Figure 1 Expected crack propagation paths for TFF (Ref. 4) (left) and TIFF (Ref. 1) (right).

Each of the calculation methods described below differ in some of the details of the above steps. Further, the applicability of the methods depends on the assumptions made and implementation details of each stage. These calculation steps could be interchanged between methods creating a number of permutations of possibilities.

Tooth flank fracture calculation methods. To the authors' knowledge, there are two main TFF load capacity calculation methods proposed in the literature.

The first model was developed by FZG. This method has been published in Witzig (Ref. 8) and Tobie, et al. (Ref. 6) and Boiadjev, et al. (Ref. 7); and relies on calculation of the local stress history based on a shear stress intensity hypothesis of Hertzter (Ref. 12). The method has significant empirical contributions and is limited in applicability due to the empirical nature of the equation used in calculating local material exposure. In the literature this method has been presented for single flank loading only; it could, in theory, be extended to consider double flank loading (i.e. idler usage), but this is not trivial. As described by Witzig, this method requires Hertzian contact stresses as inputs which can then be calculated using a gear load distribution program or via simplified analytical calculations such as those available in the standards. The method as published is also restricted to case hardened gears due to the assumptions related to the residual stress calculation. It should be noted that this method in its current form can underestimate the critical fatigue stresses if resulting residual stresses within the core are beyond negligible, since these tensile stresses within the core are currently not taken into account. This assumption for the residual stresses is only valid when the core section is much larger when compared to the thickness of the case. This introduces limitations on applicability for slender teeth and extensive case hardening depths.

Ghribi and Ocrue (Ref. 5) proposed an alternative calculation method for TFF load capacity. This method is more generic than that of Witzig (Ref. 8) and can be applied to both TFF and TIFF. The method proposes use of a multiaxial fatigue criterion and considers the importance of including tensile stresses in the core. The stress history is calculated using the Hertzian contact stress calculations of ISO/TR 15144-1 (Ref. 13) micropitting load capacity calculation standard, together with a proposal of Johnson (Ref. 14) to calculate stress at a depth inside the tooth. Method A of ISO/TR 15144-1 (Ref. 13) is based on using the results of a 3-D gear loaded tooth contact analysis, however only Hertzian contact stresses calculated by the standard have been considered in the analysis. Addition of stresses due to bending has been mentioned as planned future work, as these stresses could have an impact on the calculated stress states.

Neither of these methodologies is based on finite element analysis (FEA), although they clearly could be adapted to do so. However, using general FE packages requires considerable time and computational power to set up and run analyses.

Tooth interior fatigue fracture calculation methods. MackAldener (Refs. 1-3) has shown that an analysis method based on 2-D FEA can be utilized to analyze the risk of

TIFF and determine optimum macro geometry, material, and case hardening properties. In this analysis MackAldener used the gear load distribution analysis program *LDP (Ohio State University Load Distribution Program)* to calculate the total force on one tooth at different phases within the mesh cycle. The calculated force was then applied to a 2-D FE model of a single pair of teeth in contact as a torque after normalizing with the face width. A contact analysis was then run on the 2-D FE model in order to calculate the stress history. MackAldener's papers show the evolution of the methodology used to estimate residual stresses and material properties. While early papers (Ref. 1) described a methodology where transformation strain and material fatigue properties were assumed constant throughout the case, in later papers these assumptions were replaced with a non-homogeneous transformation strain profile and material fatigue properties that depend on the hardness profile were used within the case.

Due to the complexity of setting up and running MackAldener's FE-based method within a general FE package, MackAldener (Ref. 2) also proposed a simpler semi-analytical method. This method was proposed for rapid calculation, design parameter studies, and optimization — but with some compromise in the accuracy of the results. In the analysis of results presented in MackAldener (Ref. 2), the crack initiation risk factor result was seen to be over-predicted, as compared to MackAldener's FE-based method, by a maximum of 20%.

MackAldener used a factorial design to evaluate the effect of gear design parameters on TIFF risk and concluded that TIFF failure can be avoided if the slenderness ratio is reduced, tensile residual stresses are reduced, the gear is not used as an idler gear, and optimum case and core properties are used.

Recently Al and Langlois (Ref. 11) demonstrated a modification to the analysis of TIFF based on MackAldener's FE based method, as implemented in SMT's *MASTA* software, in which the loaded tooth contact analysis (LTCA) results from a specialized 3-D elastic contact model have been utilized to determine the load boundary conditions for TIFF analysis. This replaces a computationally expensive, explicitly modelled FE contact analysis with simple load boundary conditions obtained by a separate, specialized gear LTCA. This method has been validated against MackAldener's results and it is this method that is used throughout this paper.

In the following section the models to be used are introduced. Justification is given for model selection. The results section demonstrates the application of the described methodology as a means to investigate the risk of fatigue crack growth beneath the surface of a single flank loaded gear. Results are compared with those available within the literature (Ref. 8). Good correlation is shown for the prediction of the risk of TFF fatigue crack growth.

Methodology and Analysis

The methodology used for the analysis of TIFF and TFF has been implemented in SMT's *MASTA 7*, and previously described by Al and Langlois (Ref. 11).

MASTA's implementation is derived from MackAldener's

finite element method, but the need for a full FE tooth contact analysis has been removed by using loading conditions calculated using MASTA's specialized loaded tooth contact analysis. MackAldener also simplified his FE analysis in a later stage, not for calculation of crack initiation risk factor, but when investigating the crack propagation mechanism during the TUFF (Ref. 16). This method removes the complexity of the contact analysis and speeds up the calculation while reducing the computational requirements.

Analysis of the stress history. MASTA's 3-D loaded tooth contact analysis (LTCA) model combines an FE representation of bending and base rotation stiffness of the gear teeth and blank with a Hertzian contact formalism for the local contact stiffness. This calculation includes the effect of extended tip contact where the effective contact ratio is increased under load due to tooth bending. This effect can be particularly important for slender tooth gears that are also more at risk of TUFF.

This model is used to determine load boundary conditions at a selected number of time steps through the mesh cycle. At each time step the load distribution between and across the teeth is calculated and at each of the contact lines, load positions, load magnitudes and Hertzian half-widths are obtained.

A separate, fine 2-D mesh of the gear tooth is then built automatically, using plane strain elements. At each time step within the mesh cycle the position and distribution of the load is determined from the results of the 3-D tooth contact analysis and applied to the 2-D FE mesh using the average load position and Hertzian half-width. In the results presented below, the finite element mesh was sized according to the Hertzian half-width and a refinement study was performed to check the convergence of the results.

Hardness profile and material properties. The variation of the material properties within the case and core play an important role in TUFF; however, many assumptions have been made in previous analyses in this area. Since the analyzed gear is case hardened, the material properties are not constant throughout the tooth. The critical shear stress and fatigue sensitivity to normal stress, in the critical plane criterion, are also expected to vary with location. As with MackAldener, for our analysis we have assumed that these properties vary in the same way as an assumed hardness profile.

Hardness profile definition used by MackAldener (Ref. 3):

$$H(z) = H_{surface} \cdot g\left(\frac{z}{\bar{z}}\right) + H_{core} \cdot \left(1 - g\left(\frac{z}{\bar{z}}\right)\right) \quad (1)$$

$$g\left(\frac{z}{\bar{z}}\right) = 1 - 3 \cdot \left(\frac{z}{\bar{z}}\right)^2 + 2 \cdot \left(\frac{z}{\bar{z}}\right)^3$$

where, $H_{surface}$ and H_{core} are the hardness at the surface and core, respectively, g is a function that determines the variation

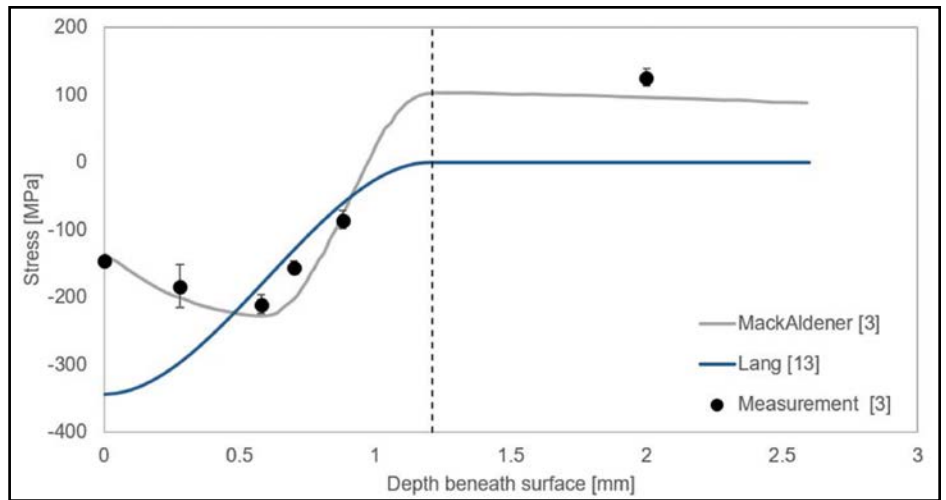


Figure 2 Experimentally measured hardness profile and curve fits of MackAldener, together with a number of empirical models available in the literature. The total case depth of 1.2 mm is marked by a dashed line; effective case depth where hardness drops below 550HV is 0.68 mm (required for empirical models). See AI and Langlois for more information.

between the case and the core defined by MackAldener, z is the normal depth at the point considered and \bar{z} is the total case depth.

This method relies on measurement of the total case depth which is often neither measured nor known. Therefore, as an alternative, a hardness measurement at a defined effective case depth is used. In such cases a different hardness profile may be utilized, i.e. Lang (Ref. 17), which in fact is the hardness profile used by Witzig (Ref. 8).

Hardness profile definition used by Lang (Ref. 17) and adopted by Witzig (Ref. 8):

$$H(z) = H_{surface} \cdot g\left(\frac{z}{CHD}\right) + H_{core} \cdot \left(1 - g\left(\frac{z}{CHD}\right)\right) \quad (2)$$

$$g\left(\frac{z}{CHD}\right) = 10^{-0.0381 \cdot \left(\frac{z}{CHD}\right) - 0.2662 \cdot \left(\frac{z}{CHD}\right)^2} \quad (3)$$

in which CHD is the effective case depth where hardness drops below 550 HV.

Comparison of hardness profile definitions. Figure 2 shows a comparison of the hardness profile measurement and curve fit proposed by MackAldener with other hardness profile models found in the literature. Unless otherwise stated, for this article MackAldener's curve fit has been used. It is interesting to note that the hardness profile model proposed by Thomas (Ref. 19) has been found to give the best comparison against MackAldener's measurement, and that of Tobe et al. (Ref. 20) is also close. The Lang method could lead to a difference in the CIRF, since fatigue properties are expected to differ near the case-core boundary.

Determination of material properties required by multiaxial fatigue analysis. In the current implementation, the material properties are assumed to vary continuously between case and core in the same manner as the hardness profile. This assumption is not required if variations of the material properties are known.

$$\sigma_{crit}(z) = \sigma_{crit,surface} \cdot g\left(\frac{z}{\bar{z}}\right) + \sigma_{crit,core} \cdot \left(1 - g\left(\frac{z}{\bar{z}}\right)\right) \quad (4)$$

$$a_{cp}(z) = a_{cp,surface} \cdot g\left(\frac{z}{\bar{z}}\right) + a_{cp,core} \cdot \left(1 - g\left(\frac{z}{\bar{z}}\right)\right) \quad (5)$$

The surface fatigue resistance of a gear flank and root can be improved by shot peening. This improvement is due to an increase in the compressive stresses in a thin layer close to the surface; this layer is very thin compared to the case hardening layer. Shot peening properties for depth and the effect on the critical shear stresses are required. In the current implementation both the depth and the effect on the critical shear stresses are assumed to be constant, the latter specified via a shot peening factor.

Residual stress analysis. Residual stresses influence the stress states within the gear tooth. These stresses are not load dependent and assumed to be constant over time. Residual stresses due to case hardening and shot peening are superimposed.

Residual stress calculation according to MackAldener:

Utilizing the 2-D mesh used to calculate the stress history due to flank loading, residual stresses are predicted by performing a separate FE analysis.

The transformation strain profile is isotropic and measured relative to the core. This profile has been presented as a piecewise polynomial with smooth connections by MackAldener (Ref. 3):

$$\varepsilon_t(z) = \begin{cases} \varepsilon_1 + 4 \cdot (\varepsilon_2 - \varepsilon_1) \cdot \left(\left(\frac{z}{\bar{z}}\right) - \left(\frac{z}{\bar{z}}\right)^2\right) & \text{if } 0 \leq z \leq \frac{\bar{z}}{2} \\ -4 \cdot \varepsilon_2 \cdot \left(1 - 6 \cdot \left(\frac{z}{\bar{z}}\right) + 9 \cdot \left(\frac{z}{\bar{z}}\right)^2 - 4 \cdot \left(\frac{z}{\bar{z}}\right)^3\right) & \text{if } \frac{\bar{z}}{2} \leq z \leq \bar{z} \\ 0 & \text{if } \bar{z} \leq z \end{cases} \quad (6)$$

where, ε_1 is the transformation strain at the surface; and, ε_2 is the maximum transformation strain.

The volume expansion in the surface layer due to the case

hardening process is modeled by applying a temperature profile to the FE model. The temperature profile applied is the same as the transformation strain profile when the coefficient of thermal expansion is set to 1. All side nodes are allowed to move only in the radial direction.

Residual stress analysis according to Lang (Ref. 17) and modified by Witzig (Ref. 8):

The calculation method proposed by Lang simply requires the heat treatment type and depth from the surface to be known in order to calculate tangential residual stresses. As can be seen from the equations, only compressive residual stresses are calculated via this method. Note that $HV(z)$ in the equation refers to Lang's hardness profile, as opposed to MackAldener's.

$$\sigma_{residual}(z) = \begin{cases} -1.25 \cdot (H(z) - H_{core}) & \text{if } H(z) - H_{core} \leq 300 \\ 0.2857 \cdot (H(z) - H_{core}) - 460 & \text{if } H(z) - H_{core} > 300 \end{cases} \quad (7)$$

This model has been used by both the TFF calculation methods proposed by Witzig (Ref. 8) and Ghribi-Octruie (Ref. 5). The implementation described by Ghribi and Octruie can, however, also calculate tensile residual stresses by considering a force balance across the teeth. (Note: this improvement on Lang's model has not been considered for this article.)

Comparison of residual stress calculation methods. Figure 3 shows the results presented by MackAldener for the variation of residual stresses with depth beneath the surface—both using the analysis method above and from measurements carried out by MackAldener. Figure 3 further compares this residual stress profile with that proposed by Lang (Ref. 17) and used by Witzig (Ref. 8) in the investigation of TFF. Interestingly, the profiles differ quite notably. This may be due to a significant material dependency not considered, but the exact reason is currently unknown and further understanding is required. It should be noted that the resulting calculated residual stresses can change from one mesh position to another due to the variation in tooth thickness.

Final stress state and fatigue crack initiation criterion.

The effective stress state within the gear teeth during its load cycle is calculated, without calculating residual stresses at each step, by superimposing the calculated stress history states and the initially estimated residual stresses.

The Findley multiaxial fatigue criterion (Ref. 18) is then used to analyze the stress history and assess the possibility of failure. Within our analysis the Findley critical plane stress has been calculated for every 5 degrees of inclination at each node. The value of 5 degrees was chosen, instead of every 1 degree used by MackAldener (Ref. 2), as results did not show a significant dependency on this value. This is confirmed by the cases presented in the results section of this paper where differences between using an inclination increment of

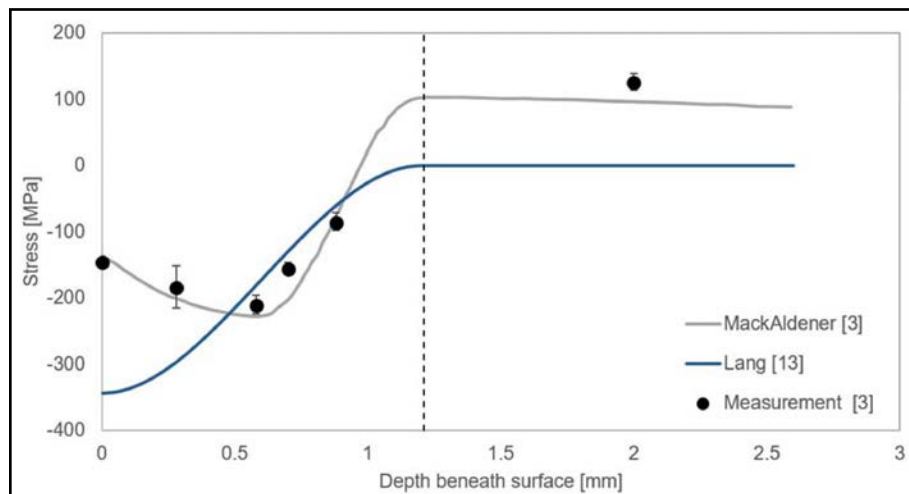


Figure 3 Variation of residual stresses with increasing depth for the original gearset defined by MackAldener. The total case depth is marked by a dashed line. See AI and Langlois for more information. The residual stress profile that is the result of the strain profile has been utilized with $=0.000833$ and $=0.00114$, as determined by MackAldener (Ref. 3).

2.5 degrees over 5 degrees is less than 0.05%.

The Findley stress is calculated as:

$$\sigma_F = \tau_a + a_{cp} \cdot \sigma_{n,max}$$

where, τ_a is the shear stress amplitude and $\sigma_{n,max}$ is the maximum normal stress.

Variation of the material properties within the tooth are related to the hardness profile, as described above.

The ratio between the maximum Findley critical plane stress and critical shear stress is a measure of the risk of crack initiation. This metric is called the crack initiation risk factor (CIRF).

Validation Results

Details of gear tooth geometries and cutters specified by Witzig (Ref. 8) are provided in Table 1. Gearset 67/69, with pressure angle 15° (details not provided here), could not be created from supplied tooth thickness and center distance information within Witzig's (Ref. 8) thesis. For each design, the CIRF throughout the tooth was calculated and trends have been compared to those obtained by Witzig (Ref. 8). Both of the gear tooth geometries used within this article do not include any profile modification other than a generous tip relief.

Estimation of material fatigue properties for Findley multi-axial fatigue criterion. Fatigue properties of the core and surface material required for Findley multi-axial fatigue criterion were estimated. Fatigue sensitivity to normal stress was assumed 0.3 within the core, and 1 at the surface. The local material shear strength definition used by Witzig (Ref. 8) — $\tau_{crit} = 0.4 \cdot HV(z)$ — was used. The calculation of the Findley critical shear stress has been carried out according to MackAldener (Ref. 3).

Estimation of transformation strains for MackAldener's residual stress calculation. MackAldener (Ref. 3) gives a clear description of how transformation strain values can be estimated at the surface, and the mid-case depth using two residual stress simulations. First, simulation with transformation strain 1 on the surface and 0 at the mid-case depth was performed. The surface stress calculated by Lang (Ref. 17) was then compared to the calculated residual stress; linear interpolation was used to calculate the transformation strain at a surface point leading to the surface stress of Lang. A similar analysis was carried out at the mid-total case depth. The transformation strain profile definitions used within the current analysis are provided in Table 2.

Analysis Results

Witzig (Ref. 8) has run numerous experiments with test gears and validated their calculation model, suggesting a critical value of 0.8 for material exposure. These gearsets were designed to fail due to tooth flank fracture, and results were reproducible. It is important to note that failure analysis of these gearsets showed that, in the majority of cases, initial crack initiation occurred at an inclusion near the case-core boundary. However, the size and

Spur gear set designation	40/41		67/69	
	Pinion	Wheel	Pinion	Wheel
Number of teeth	40	41	67	69
Centre distance [mm]	200		200	
Module [mm]	5		3	
Pressure angle [°]	20		20	
Profile shift coefficient	-0.23	-0.2456	-0.61	-0.6169
Tip diameter [mm]	205.6	210.2	201.2	207.16
Face width [mm]	18	18	18	18
Number of teeth measured for chordal span	5	5	7	6
Average chordal span measured [mm]	68.287	68.304	59.02	50.237
Assumed finish stock [mm]	0.04	0.04	0.04	0.04
Normal thickness of the cutter [mm]	7.854		4.712	
Protuberance [mm]	0.2		0.15	
Protuberance height [mm]	2.853		1.383	
Addendum for cutter [mm]	7.4		4.71	
Dedendum for cutter [mm]	5.6		4.54	
Cutter tip edge radius [mm]	2		0.81	
Cutter fillet radius [mm]	1		0.6	
Core Hardness HV	405		410	
Surface Hardness HV	695		695	
Effective Case Depth, HV550 [mm]	0.69		0.5	

Spur gear set designation	40/41		67/69	
	Surface, ϵ_1	Mid-case, ϵ_2	Surface, ϵ_1	Mid-case, ϵ_2
Transformation strain	0.000609	0.001163	0.000618	0.00121
Estimated total case depth	1.38 mm		0.98 mm	
Critical stress at surface	235 MPa			
Critical stress in core	675 MPa			

effect of these inclusions are not included within the analysis in that the material is considered homogeneous.

Figure 4 summarizes the results from Witzig (Ref. 8) for spur gear set 40/41 (Fig. 4a) and 67/69 (Fig. 4b). It should be noted that the y-axis on the right, for the maximum material exposure, is shifted to give comparable results, as the critical value for the Findley criterion is expected to be 1 and 0.8 for Witzig.

Figure 4 also shows the calculated CIRF using the proposed methodology with and without tensile residual stresses. Although not clearly seen in the figure, the gradient of calculated crack initiation risk factor, with respect to torque, grew by 10.9%, and 11.8% when residual tensile stresses are included for spur gearset 40/41 and 67/69, respectively. Further, the gradient of a line fit of the results obtained by Witzig is found to be lower than that for the proposed method.

Witzig (Ref. 8) has observed that experimental test gears fail when maximum material exposure exceeds 0.8, but this value does not consider the effect of the inclusion on the stress field. Therefore further understanding of CIRF-initiated TFF failure is required.

Given the assumptions made — including the assumption that a critical CIRF of 1 can be compared with a maximum material exposure of 0.8 — the results obtained show similar qualitative behavior, but also some significant difference in the torque, which leads to the critical metric values. Further investigation is required to understand whether this difference is down to the assumptions made in our inputs or a more fundamental difference in the formalism of the methods.

Figure 5 shows a comparison of experimental failure shapes from (Ref. 8) and crack initiation points with calculated crack

initiation risk factors from the proposed method for both residual stress calculation methods considered. It should be noted that experimental failures originated from inclusions which act as stress concentration regions. Therefore the calculated maximum crack initiation risk factor may not necessarily coincide with the experimental crack initiation point. Figure 5 does, however, show good correlation between the position of crack initiation in the tests and the calculated region of high CIRF.

Furthermore, results show that the area with the highest crack initiation risk is smaller when tensile residual stresses are considered due to the profile of the residual tensile stresses into the tooth i.e. — highest risk is within the case-core boundary.

Conclusions

Application of an FEA-based analysis technique to analyze risk of TIFF crack initiation has been applied to TFF, with results presented and compared against open literature.

The conclusions from this paper are as follows:

- It is possible to analyse the risk of tooth fatigue fracture by applying a methodology based on MackAldener where computationally expensive, explicitly modelled, FE-based contact analysis is replaced with simple load boundary conditions obtained by a separate, specialized gear-loaded tooth contact analysis.
- It has been shown that there is a linear relationship between torque and material exposure, as calculated by Witzig, within the range investigated. A linear relationship has also been observed between torque and calculated crack initiation risk factor.
- As is to be expected, thresholds obtained from Witzig's calculation method and Findley are different. The critical value has been found to be close to 1, but requires further investigation.
- The calculated crack initiation risk factor is higher when residual stresses are estimated with MackAldener (i.e. when tensile residual stresses are considered within the core), compared to Lang. It has been found that the effect of the residual stresses increases with torque.
- Further studies are required to evaluate thresholds and material properties used within different fatigue criteria.

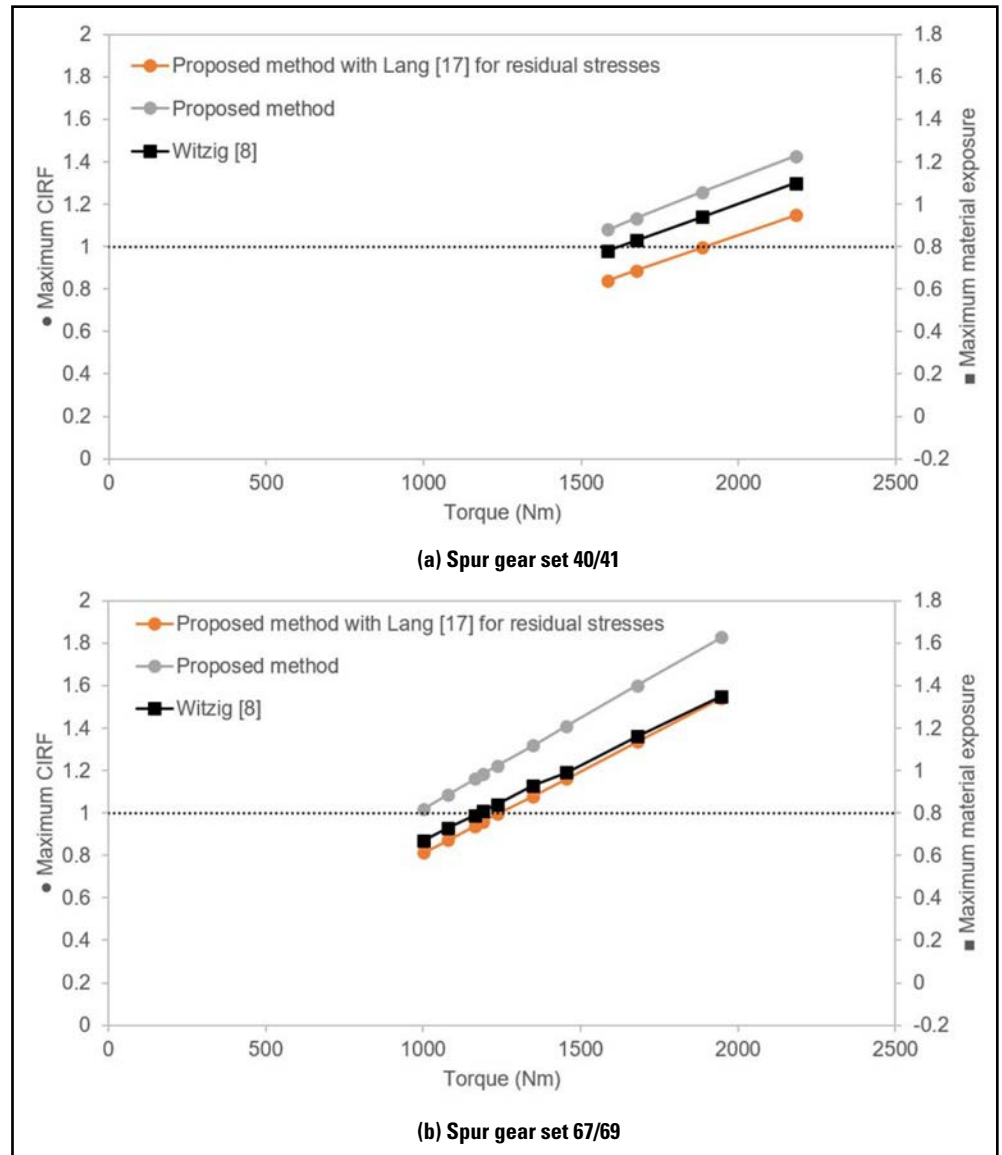



Figure 4 Comparison of the calculated maximum CIRFs from MASTA and Witzig's (Ref. 8) method. It should be noted that the y-axis of the maximum material exposure is shifted to give comparable results (i.e., critical value for Findley criterion is expected to be 1, and 0.8 for Witzig). The dotted line represents the expected critical value for the fatigue criterion used.

Further work on comparison of TIFF and TFF load carrying capacity with other failure modes, such as bending and pitting fatigue, are planned for future work.

It is the authors' opinion that the critical effect of material quality and inclusions is the key factor missing in the types of analyses previously presented. We would expect that this could be addressed as a factor applied to, for example, the material thresholds; however, significant field experience and further experimental studies are required to address this point. 

References

1. MackAldener, M. and M. Olsson. "Interior Fatigue Fracture of Gear Teeth, Fatigue & Fracture of Engineering Materials & Structures," 23 (4), 2000, pp. 283-292.
2. MackAldener, M. and M. Olsson. "Design Against Tooth Interior Fatigue Fracture," *Gear Technology*, Nov/Dec 2000, pp.18-24.
3. MackAldener, M. and M. Olsson. "Tooth Interior Fatigue Fracture," *International Journal of Fatigue*, 2001, 23, pp. 329-340.
4. Bauer, E. and A. Bohl. Flank Breakage on Gears for Energy Systems, VDI

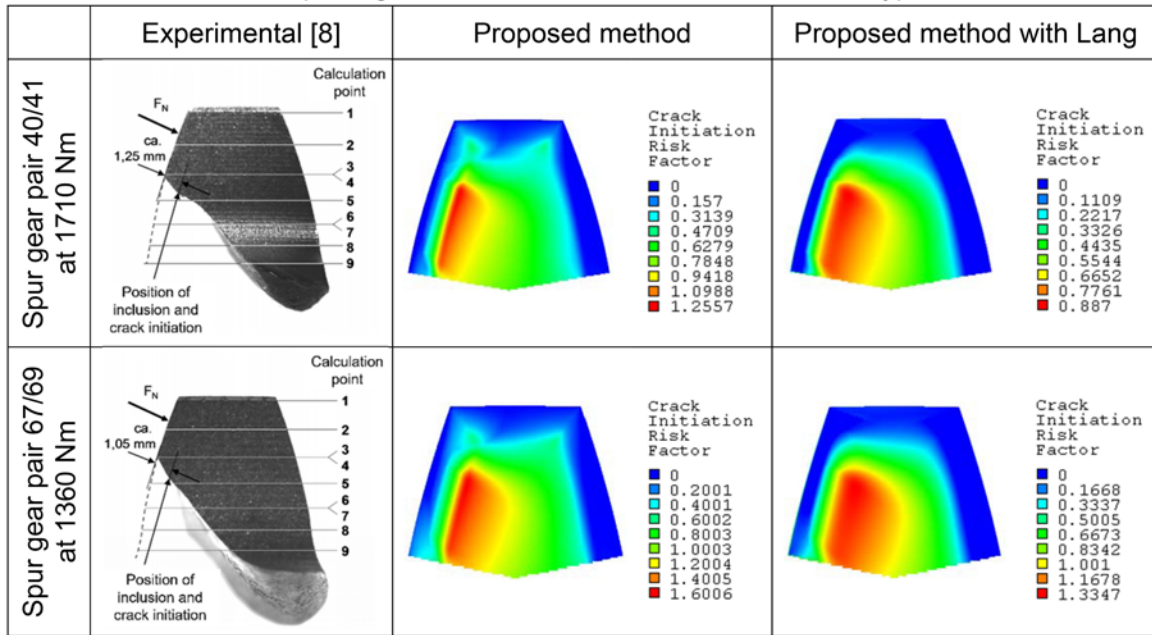


Figure 5 Comparison of experimental failure shape (Ref. 8) and calculated crack initiation risk factor; CIRF for both residual stress calculation methods considered.

International Conference on Gears, October 2010; also *Gear Technology*, November/December 2011.

5. Ghribi, D. and M. Octrue. "Some Theoretical and Simulation Results on the Study of the Tooth Flank Breakage in Cylindrical Gears," *International Gear Conference*, Lyon, France, 26-28, August 2014.
6. Tobie, T., B.-R. Höhn and K. Stahl. "Tooth Flank Breakage — Influences on Subsurface- Initiated Fatigue Failures of Case Hardened Gears," *Proceedings of the ASME 2013 Power Transmission and Gearing Conference*, Portland, OR, August 2014.
7. Boiadjev, I., J. Witzig, T. Tobie and K. Stahl. (2014) "Tooth Flank Fracture — Basic Principles and Calculation Model for a Sub-Surface-Initiated Fatigue Mode of Case Hardened Gears," *International Gear Conference*, Lyon, France 26-28, August 2014; *Gear Technology*, August 2015.
8. Witzig, J. "Flankenbruch Eine Grenze der Zahnradtragfähigkeit in der Werkstofftiefe," PhD Thesis, Technical University of Munich, 2012.
9. BS ISO 6336-1. Calculation of Load Capacity of Spur and Helical Gears — Part 1: Basic Principles, Introduction and General Influence Factors, 2006.
10. ANSI/AGMA 2101-D04. Fundamental Rating Factors and Calculation Methods for Involute Spur and Helical Gear Teeth, 2004.
11. Al, B. and P. Langlois. "Analysis of Tooth Interior Fatigue Fracture Using Boundary Conditions form an Efficient and Accurate Loaded Tooth Contact Analysis," British Gears Association (BGA) *Gears 2015 Technical Awareness Seminar*, 12th of November 2015; *Gear Solutions* February 2016.
12. Hertter, T. "Rechnerischer Festigkeitsnachweis der Ermüdungstragfähigkeit Vergüteter und Einsatzgehärteter Zahnräder," PhD Thesis, 2003, Technical University of Munich.
13. BS ISO/TR 15144-1:2014. Calculation of Micropitting Load Capacity of Cylindrical Spur and Helical Gears — Part 1: Introduction and Basic Principles.
14. Johnson, K. L. *Contact Mechanics*, Cambridge University Press, 1985, Oxford, UK.
15. MackAldener, M. and M. Olsson. "Analysis of Crack Propagation during Tooth Interior Fatigue Fracture," *Engineering Fracture Mechanics*, 2002, 69, pp. 2147-2162.
16. MackAldener, M. and M. Olsson. "Analysis of Crack Propagation during Tooth Interior Fatigue Fracture," *Engineering Fracture Mechanics*, 69, 2002, pp. 2147-2162.
17. Lang, O. R. "The Dimensioning of Complex Steel Members in the Range of Endurance Strength and Fatigue Life," *Zeitschrift fuer Werkstofftechnik*, 1979, Vol. 10, p.24-29.
18. Findley, W. N. "A Theory for the Effect of Mean Stress on fatigue of metals under combined torsion and axial load or Bending," 1959, *Journal of*

Engineering for Industry, pp. 301-306.

19. Thomas, J. "Flankentragfähigkeit und Laufverhalten von Hartfeinbearbeiteten Kegelrädern," 1997, PhD Thesis, Technical University of Munich, Germany.
20. Tobe, T., M. Kato, K. Inoe, N. Takatsu and I. Morita. "Bending Strength of Carburized C42OH Spur Gear Teeth," *JSME*, 1986, p. 273-280.

Baydu Al has been an analyst software engineer at Smart Manufacturing Technology (SMT) since October 2014. Prior to joining SMT he worked as a researcher at Nottingham University (gas turbine and transmission systems), specializing in efficiency and oil management. Since joining SMT Al has been busy contributing to MASTA's loaded tooth contact analysis, and analysis of tooth interior fatigue fracture.



Dr. Rupesh Patel has since January 2016 worked at Smart Manufacturing Technology (SMT) as a systems analyst/software developer. During this time he has been actively involved in research and development of functionality for the analysis of tooth interior fatigue fracture and for gear macro-geometry optimization. Prior to employment at SMT, Patel worked for several years as a post-doctoral researcher at the University of Nottingham, specializing in structural dynamics and focusing on energy harvesting from natural sources of vibration. Patel was also employed in Japan in relation to this work and has published numerous scientific papers over his career.



Dr. Paul Langlois is the CAE products development department manager at SMT. Having worked for SMT for 10 years, he has extensive knowledge of transmission analysis methods and their software implementation. He manages the development of SMT's software products and is a main contributor to many aspects of the technical software development. As a member of the BSI MCE/005 committee, Langlois contributes to ISO standards development for gears.



For Related Articles Search

failure

at www.geartechnology.com